

Initial growth of single-walled carbon nanotubes on supported iron clusters: a molecular dynamics study

H. Duan^{1,a}, F. Ding², A. Rosén¹, A. Harutyunyan³, T. Tokune³, S. Curtarolo⁴, and K. Bolton^{1,5}

¹ Physics Department, Göteborg University, 412 96 Göteborg, Sweden

² ME&MS Department, Rice University, Houston, TX 77005, USA

³ Honda Research Institute USA Inc., Columbus, OH 43212, USA

⁴ ME&MS, Duke University, Durham, NC 27708, USA

⁵ School of Engineering, University College of Borås, 501 90 Borås, Sweden

Received 27 July 2006 / Received in final form 29 September 2006

Published online 24 May 2007 – © EDP Sciences, Società Italiana di Fisica, Springer-Verlag 2007

Abstract. Molecular dynamics simulations were used to study the initial growth of single-walled carbon nanotubes (SWNTs) on a supported iron cluster (Fe_{50}). Statistical analysis shows that the growth direction of SWNTs becomes more perpendicular to the substrate over time due to the weak interaction between carbon nanotube and the substrate. The diameter of the nanotube also increases with the simulation time and approaches the size of the supported iron cluster.

PACS. 31.15.Qg Molecular dynamics and other numerical methods – 61.46.-w Nanoscale materials

1 Introduction

Since their discovery [1], carbon nanotubes (CNTs) have attracted great interest due to their special physical and chemical properties and large range of potential applications. Some applications, like field-emission or electronic devices, need large-scale aligned growth of CNTs. There are many methods to produce aligned CNTs in chemical vapour deposition (CVD) experiments, such as using flowing source feedstock gases [2–6], electric fields [7–9], magnetic fields [10], soft-lithography [11] or combinations of them [12]. Preparation of the catalytic cluster/particle and substrate is crucial in all of these methods. The catalytic particle plays a critical role in the initial nucleation of CNTs, and the growth of aligned CNTs is governed, among other things, by the interaction of the substrate with the metal catalyst and the CNT, resulting in vertical [3,11], horizontal [6] or other laterally aligned CNTs [4,5,9,10]. In this work, we present a study of the initial growth of single-walled carbon nanotubes (SWNTs) on supported iron catalysts to understand the influence of the catalytic particle and substrate on SWNT growth.

2 Force field and simulation method

The force field adopted here is based on that used to study SWNT growth from free iron clusters, and a detailed de-

scription appears elsewhere [13,14]. Briefly, a many-body potential [15], which is based on the second moment approximation of the tight-binding model [16,17], was used for the interaction between iron atoms. It is known that this potential is suitable for studying the thermal properties of pure and alloy transition metal systems. The interaction between carbon atoms is either the Lennard-Jones type (LJ) [18] or the Brenner model [19] depending on if the atoms are dissolved inside the cluster or precipitated on its surface, respectively. The interaction between iron and dissolved carbon atoms is modeled by the Johnson potential [20], which gives the correct trend for the iron-carbide phase diagram and the correct dependence of cluster melting point on cluster size [14]. The interaction between iron and precipitated carbon atoms was fit to density-functional theory (DFT) energies and geometries [13].

To simulate SWNT growth from *supported* clusters, the interaction with the substrate is divided into two types; one for the iron and dissolved carbon atoms and the other for the precipitated (Brenner) carbon atoms. A Morse type potential was used for the former since this provided the best fit to DFT energies and geometries of iron-carbide clusters supported on an aluminium oxide substrate [21]: $D[e^{-2\alpha(z-z_0)} - 2e^{-\alpha(z-z_0)}]$, with parameters $D = 0.153$ eV, $\alpha = 1.268$ Å⁻¹ and $z_0 = 2.219$ Å. As described previously [21], these parameters are used for both the iron and dissolved carbon atoms, and the growth

^a e-mail: haiming.duan@physics.gu.se

mechanism does not depend on moderate changes (up to 20% has been tested) in the substrate-carbon parameters.

As far as we are aware there are no published force fields for the interaction between CNTs (or graphene layers) and substrates like aluminium oxide. Since this interaction is expected to be rather weak, we used an available model for C_{60} -graphene interactions, where the authors adopt a Lennard-Jones type potential and the interaction parameters are determined from experiment [22]: $A/r^{12} - B/r^6$, with $A = 22500 \text{ eV } \text{\AA}^{12}$ and $B = 15.4 \text{ eV } \text{\AA}^6$. This is a very weak interaction of about 2.635 meV per carbon atom. In this work we also study the effect of increasing this interaction strength on the growth mechanism.

The constant temperature molecular dynamics method was used to study the growth of SWNTs on supported Fe_{50} clusters. A total of 120 trajectories were propagated to ensure converged statistics of the change in growth direction and SWNT diameter over time. The temperature (1000 K in this study) was controlled by the Berendsen thermostat [23] and the integration time step is 1 fs. Briefly, the Fe_{50} cluster (diameter of about 1 nm) was heated to 1000 K before carbon atoms were added into the iron cluster at a constant rate of one carbon atom per 40 ps. This is faster than experimental addition rates, but decreasing the addition rate does not affect the growth mechanisms discussed here. Several iron atoms (6 in this study) were fixed to the substrate to avoid the possibility of the iron-carbide cluster lifting off the substrate due to the formation of a graphene layer between iron-carbide cluster and the substrate.

3 Results and discussion

The nucleation mechanism of SWNTs on supported Fe_{50} clusters is similar to that on free Fe_{50} clusters reported previously [13]. Once the cluster is highly supersaturated in carbon, the dissolved carbon atoms precipitate on the surface. These atoms form graphitic islands that lift off the cluster as caps that elongate into SWNTs [13]. It can be noted that there is some debate as to whether carbon dissolves into small iron clusters like Fe_{50} [24], but this does not affect the cap and SWNT growth mechanism presented here, which occurs from the carbon atoms on the cluster surface.

Figures 1a and 1b show two typical snapshots of SWNT cap growth at 4.5 and 6.7 ns after the first carbon atom is added to the Fe_{50} cluster. At 4.5 ns the cap diameter is about 0.7 nm, and increases to approximately 1 nm at 6.7 ns, which is similar to the cluster diameter. Two points about the defects of SWNTs should be mentioned in this growth process. First, from Figure 1 we can see that, in addition to the heptagons and pentagons which are required to form a perfect tube cap, there are many other polygons in the nanotube and, second, there are defect carbon atoms inside the nanotube. There are several possible reasons for these defects, such as the short simulation time (compared with experiment) which may not allow for annealing to the minimum energy structure and

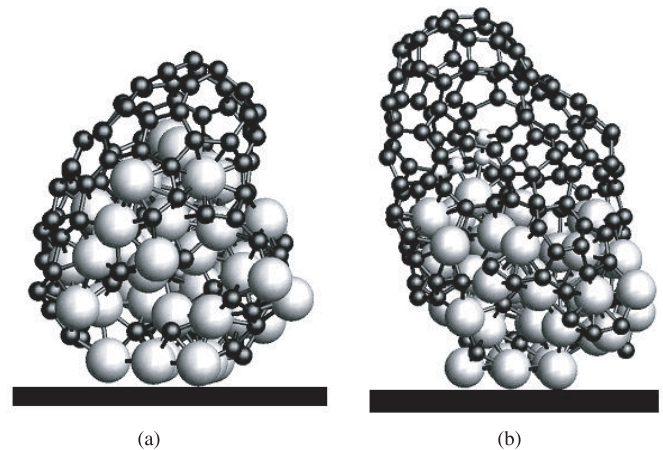


Fig. 1. Snapshots of typical SWNT caps at 4.5 ns (a) and 6.7 ns (b). Iron atoms are shown as big spheres and carbon as small ones. The inner carbon atoms (grey) shown in (b) are defects inside the tube. The black basis panel denotes the substrate.

inaccuracies in the force field [19]. These defects are similar to those found when simulating SWNT growth on free iron clusters and have been discussed elsewhere [13].

Figure 2 shows the average growth angle of the SWNT caps relative to the substrate at 4.50 and 6.70 ns. There is a shift from an almost random distribution with a small peak at 40–50 degrees to a preferred angle of 50–70 degrees. Hence, the growth of the cap becomes more perpendicular with increasing time. The increase of nanotube growth angle with time is due to the interactions between the carbon atoms and the substrate. Dissolved carbon atoms are more strongly attracted to the substrate (0.153 eV per atom) and have a smaller equilibrium distance from the substrate (0.22 nm) than the precipitated carbon atoms (2.635 meV per atom and 0.38 nm, respectively). Since there are more precipitated carbon atoms with increasing time and these atoms cover more of the cluster surface, their larger equilibrium distances repel them from the substrate and the growth angle increases.

Figure 3 gives the average cap diameters at 4.50 and 6.70 ns. The average diameter increases with time from 0.8–0.9 nm at 4.5 ns to 0.9–1.1 nm at 6.7 ns. The latter range is similar to the diameter of the iron-carbide cluster. This linear relationship between SWNT and cluster diameter has been observed experimentally [25] and, as discussed previously [26], is expected since it maximises the SWNT/cap — cluster interaction strength.

Since the substrate interaction is important for the growth of carbon nanotubes, we repeated the above simulations but with different substrate interaction strengths and equilibrium distances. These simulations include: (a) increasing the iron-substrate interaction strength by 20%, (b) increasing the Brenner carbon-substrate interaction strength by 200 and 500%, (c) reducing and increasing the dissolved carbon-substrate interaction strength by 20%. All results are similar to those described above, except

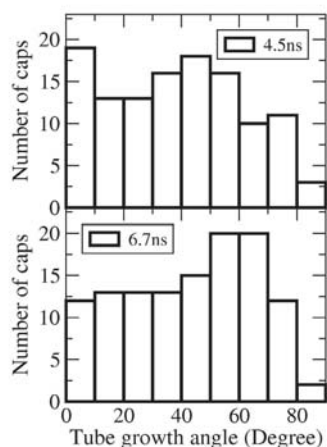


Fig. 2. Distribution of the growth angle of SWNT caps at 4.5 ns (upper panel) and 6.7 ns (lower panel). The total number of SWNT caps is 120.

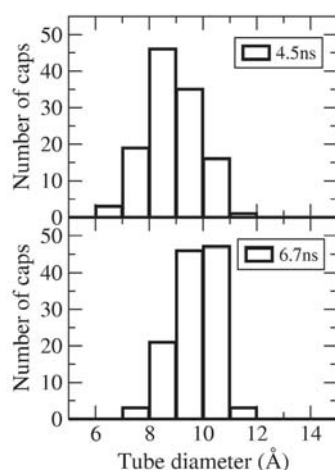


Fig. 3. Distribution of SWNT cap diameters at 4.5 ns (upper panel) and 6.7 ns (lower panel). The total number of SWNTs is 120.

when increasing the Brenner carbon-substrate interaction strength by 500%, where the cap does not show a strong preference for perpendicular growth at long times. This is expected since, for very large SWNT-substrate interactions, horizontal SWNT growth may be preferred [27].

The model used in this work can potentially be used to study the growth and properties of a variety of carbon structures. For example, encapsulation of free metal particles and growth of bamboo and soot-like structures have been studied [13,28]. However, the Brenner potential does not contain C-C non-bonded interactions, and hence multi-walled CNTs cannot be studied. In addition, this potential is known to underestimate the energy of defect formation in SWNT walls [29], which provides a possible explanation for the multiple defects seen in the simulated SWNT structures (Fig. 1) and hinders studies of

more complex carbon structures such as schwarzite [30]. A modified Brenner potential [31], called the adaptive intermolecular reactive empirical bond-order model (AIREBO) includes C-C non-bonded interactions and preliminary studies show that it also yields improved defect energies, and thus may be preferred when studying structural properties of carbon materials. Also, effects of charging the substrate, which is known to effect the rate of CNT growth [32] and which may lead to a distribution of charge along the SWNT, cannot be modelled using the (modified) Brenner potential.

4 Conclusion

The initial growth of SWNTs on a supported Fe_{50} cluster was studied by molecular dynamics simulations. Over one hundred simulations were performed in order to get converged statistics. It is found that, with increasing time, the average SWNT cap growth direction relative to substrate becomes more perpendicular due to the weak interaction between the cap and the substrate and the relatively large cap-substrate equilibrium distance. The diameter of the nanotube also increases and approaches the size of the catalytic particle. Stronger SWNT-substrate interaction leads to growth that does not show a strong preference for perpendicular directions.

The authors are grateful for time allocated on the Swedish National Supercomputing facilities. Financial support was obtained from the Swedish Research Council, the Swedish Foundation for Strategic Research (CAMEL consortium) and The Honda Research Institute, Inc.

References

1. S. Iijima, *Nature* **354**, 56 (1991)
2. Y. Chen, J. Yu, *Carbon* **43**, 3181 (2005)
3. S. Noda, H. Sugime, T. Osawa, Y. Tsuji, S. Chiashi, Y. Murakami, S. Maruyama, *Carbon* **44**, 1414 (2006)
4. S. Orlanducci, V. Sessa, M.L. Terranova, M. Rossi, D. Manno, *Chem. Phys. Lett.* **367**, 109 (2003)
5. S. Huang, X. Cai, C. Du, J. Liu, *J. Phys. Chem. B* **107**, 13251 (2003)
6. L. Huang, X. Cui, B. White, S.P. O'Brien, *J. Phys. Chem. B* **108**, 16451 (2004)
7. Y. Chen, D.T. Shaw, L. Guo, *Appl. Phys. Lett.* **76**, 2496 (2000)
8. C. Chiu, N.H. Tai, M.K. Yeh, B.Y. Chen, S.H. Tseng, Y.H. Chang, *J. Cryst. Growth* **290**, 171 (2006)
9. E. Joselevich, C.M. Lieber, *Nano. Lett.* **2**, 1137 (2002)
10. K.H. Lee, J.M. Cho, W. Sigmund, *Appl. Phys. Lett.* **82**, 448 (2003)
11. S. Huang, A.W.H. Mau, T.W. Turney, P.A. White, L. Dai, *J. Phys. Chem. B* **104**, 2193 (2000)
12. C.M. Hsu, C.H. Lin, H.L. Chang, C.T. Kuo, *Thin Solid Films* **420-421**, 225 (2002)
13. F. Ding, K. Bolton, A. Rosén, *J. Phys. Chem. B* **108**, 17369 (2004)

14. F. Ding, K. Bolton, A. Rosén, *J. Vac. Sci. Technol. A* **22**, 1471 (2004)
15. J. Stanek, G. Marest, H. Jaffrezic, H. Binczycka, *Phys. Rev. B* **52**, 8414 (1995)
16. V. Rosato, M. Guillope, B. Legrand, *Philos. Mag. A* **59**, 321 (1989)
17. R.P. Gupta, *Phys. Rev. B* **23**, 6265 (1981)
18. J.H. Walther, R. Jaffe, T. Halicioglu, P. Koumoutsakos, *J. Phys. Chem. B* **105**, 9980 (2001)
19. D.W. Brenner, *Phys. Rev. B* **42**, 9458 (1990)
20. R.A. Johnson, *Phys. Rev.* **134**, A1329 (1964)
21. A. Jiang, N. Awasthi, A.N. Kolmogorov, W. Setyawan, A. Börjesson, K. Bolton, A. Harutyunyan, S. Curtarolo, *Phys. Rev. B* (accepted)
22. H. Ulbricht, G. Moos, T. Hertel, *Phys. Rev. Lett.* **90**, 095501 (2003)
23. H.J.C. Berendsen, J.P.M. Postma, W.F. van Gunsteren, A. DiNola, J.R. Haak, *J. Chem. Phys.* **81**, 3684 (1984)
24. J.-Y. Raty, F. Gygi, G. Galli, *Phys. Rev. Lett.* **9**, 096103 (2005)
25. A.M. Cassell, J.A. Raymakers, J. Kong, H. Dai, *J. Chem. Phys.* **103**, 6484 (1999)
26. F. Ding, A. Rosén, K. Bolton, *J. Chem. Phys.* **121**, 2775 (2004)
27. H. Ago, K. Nakamura, K. Ikeda, N. Uehara, N. Ishigami, M. Tsuji, *Chem. Phys. Lett.* **408**, 433 (2005)
28. F. Ding, K. Bolton, A. Rosén, *J. Elec. Mat.* **35**, 207 (2006)
29. F. Ding, *Phys. Rev. B* **72**, 245409 (2005)
30. S.J. Townsend, T.J. Lenosky, D.A. Muller, C.S. Nichols, V. Elser, *Phys. Rev. Lett.* **69**, 921 (1992)
31. S.J. Stewart, A.B. Tutein, J.A. Harrison, *J. Chem. Phys.* **112**, 6472 (2000)
32. N.M. Bulgakova, A.V. Bulgakov, J. Svensson, E.E.B. Campbell, *Appl. Phys. A* **85**, 109 (2006)